FLOW CHARACTERISTICS OF BACKWARD CURVED CENTRIFUGAL FAN WITH RECTANGULAR CASING

Hidechito HAYASHI[1], Kyohei NAKAMURA[2], Souichi SASAKI[1]
Seiji SHIRAHAMA[3], Atsushi NAGATA[3]

[1] *Nagasaki Univ., System Science division, 1-14 Bunkyo machi, Nagasaki, Japan*

[2] *Graduate School of Nagasaki Univ., 1-14 Bunkyo machi, Nagasaki, Japan*

[3] *Panasonic Eco Systems Ltd., 4017 Takaki cho, Kasugai, Japan*

SUMMARY

The flow characteristics for the backward curved centrifugal fan were investigated with experiments and simulations. The length of the casing was varied. It was cleared that the performance of the fan is decreased and the noise level is increased with the casing. The pressure in the casing varies with the section area of the casing. The pressure is low at the small section area between the casing wall and the impeller outlet. The pressure at the impeller outlet varies mainly with the distortion of the outflow from the impeller. It is low near the outlet of the fan because of the large outflow from the impeller. When the outflow increases, the pressure becomes low at the outlet of the impeller. The discrete frequency noise from the fan is mainly generated by the interaction of the distorted outflow and the blades.

INTRODUCTION

The backward curved centrifugal fans are used in the air conditioner, ventilation system and air-cleaner. This type of fan generates the high pressure with high efficiency and low noise. The centrifugal fan is usually equipped with the scroll casing, which effectively collects the energy that is generated in the impeller. But the fan with scroll casing needs the large space. The performance curve of it is steeply decreased with the flow rate. The interaction noise with the tongue of scroll casing becomes large. Then it is required to small, gentle performance and lower noise[1]-[4]. For the small fans, the fan is not used the scroll casing recently. Though the energy out of the impeller is not collected effectively, it seems hardly to obtain the high efficiency and the large pressure rise. But it is not clear. The performance of the fan is expected to be varied with casing geometry[5]-[9]. The dynamics of the flow in the fan is much varied with the interaction between the impeller and the casing.

In this report, it is pointed out the effects of the casing for the fan performance. The rectangular casing is examined with comparing to the without casing fan. Then numerical simulation and the experiments for the performance are made. The distorted flow characteristics and the influence to performance are shown.

EXPERIMENTS AND SIMULATION CONDITIONS

Performance Test Apparatus

The Test Apparatus is shown in figure 1. The two anechoic chambers, the intake and the exhaust chambers, are used to the inlet and outlet sides of the fan. The dimensions of the intake and exhaust chambers are 4500D*4200W*2500H and 3000D*4200W*2500H, respectively. The chambers are connected with the squared duct, which is 100 0 mm square. The test fan is set the connecting duct. The background noise of each chamber is 17dB. The air circulates in the chambers. The booster fan and the flow measuring equipment are in the control and measurement unit. The booster fan and the air conditioner are set to keep the flow and temperature. The air out of the air conditioner flows to the intake chamber again.

Figure 2 shows the impeller of the examined fan. The outer and inner diameters are 230 mm and 140 mm. The eye diameter of the upper shroud is 144mm, a little larger than the inner diameter. The leading edge of the blade is not covered with the upper shroud. The span is 61 mm at the outlet of the impeller. The blade is made of the two dimensional plate. The number of blades is 7. The rotating speed of the impeller is 1100 rpm. The ratio of the inner and outer diameter is 0.62 and the area ratio is 0.37. These ratios are a little small compared to the ordinary centrifugal fan.
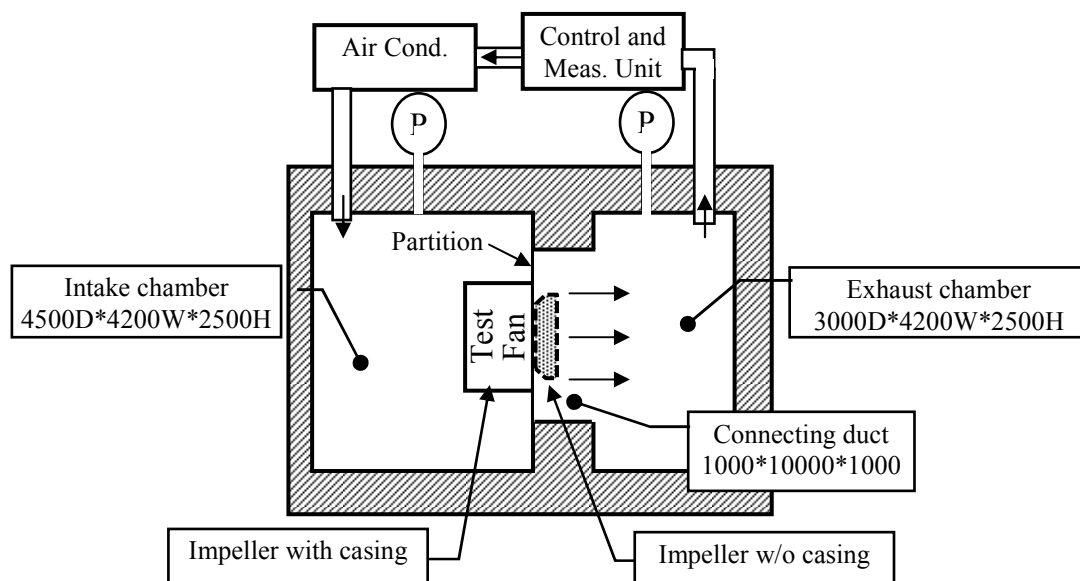

Figure 1: Experimental apparatus

The fan is tested for without casing and two type casings. The performance and noise characteristics are measured in experiments. At the without casing test, the bell-mouth is set to the partition directly and the air out of impeller flows directly in connecting duct. At the casing test, the fan is in the intake chamber and the outlet of the casing is connected to the partition. Figure 3 shows the two type casings. The casing shown in figure (a) has the squared casing. The dimension of the casing is 350W*350D*158H mm. It is called C350 in this paper. The impeller is set at the center of the casing. The distance between the impeller and the casing is 60 mm. Figure (b) is the rectangular casing. The dimension of the casing is 350W*550D*158H mm. The length of the casing is 200 mm

longer than C350 casing. Other dimensions are same to C350. It is called C550 in this paper. The location of the impeller is same as the distance from the back wall of the casing of C350.

The airflow rate is measured by the Venturi meter which is equipped in the control and measuring unit. The pressure rise of the test fan is measured by the pressure difference between the intake and exhaust chambers. Each pressure is averaged of four pressure taps at the wall. The power of the fan is measured from the input power of the motor.

Figure 2: test impeller

The flow characteristics in the fan are investigated by the numerical simulation. The simulation is made with the same condition as the experiments. Figure 4 shows the numerical simulation region. The exhaust region is corresponding to the connecting duct of the experiments. The boundary conditions are set for the inlet velocity and the outlet pressure. The number of the elements is about 3,000,000 which are unstructured tetra mesh. The turbulent model is SST. The steady and unsteady flows are simulated.
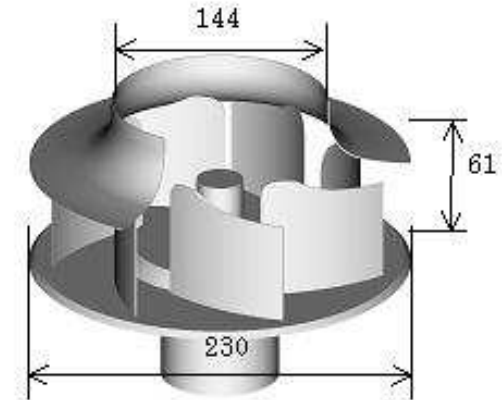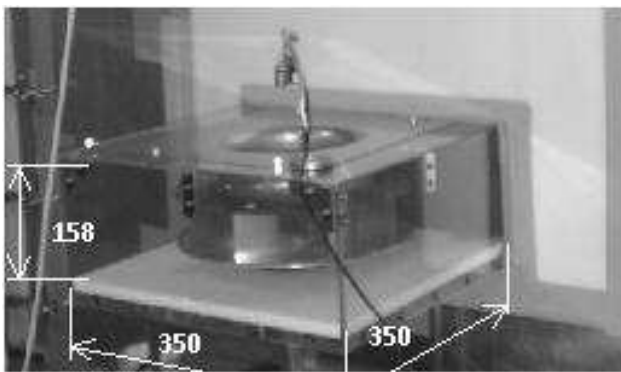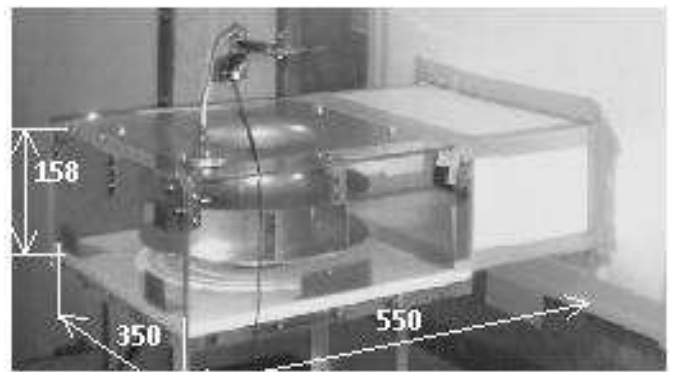

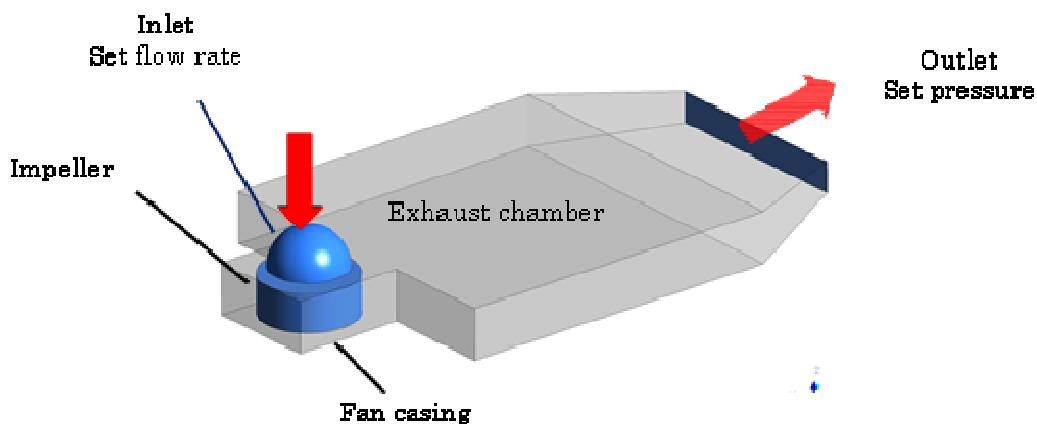| (a) C350 (350*350*158) squared casing | (b) C550 (350*550*158) rectangular casing |

Figure 3: Schematics of test fans

Figure 4: Simulated fan and domain

RESULTS AND DISCUSSIONS

Performances of Fan

Figure 5 shows the performance curves. The values are normalized at the condition of the maximum efficiency point of the without casing fan (w/o casing). Figure (a) is the variation of the static pressure with the flow rate. The pressures of all fans are gradually decreased with the flow rate. The pressures of the C350 and C550 fans are about 0.2 lower than the w/o casing fan in the large flow rate. But the length of the casing is hardly influenced to the static pressure. Figure (b) shows the efficiency curves. The efficiencies of C350 and C550 are about 10 percent lower than the w/o casing fan. The flow rate at the maximum efficiency is a little smaller than the w/o casing fan. The efficiencies of C350 and C550 fans are almost the same. It is seemed that the loss of the fan is mainly generated in the impeller and near the back wall of the casing.

Figure 6 is the distribution of the sound pressure level. The SPL(A) is increased with the flow rate. The level of the noise of C350 and C550 is 3 to 5 dB larger than the without casing fan. The difference between C350 and C550 is caused by the resonance of the casing.
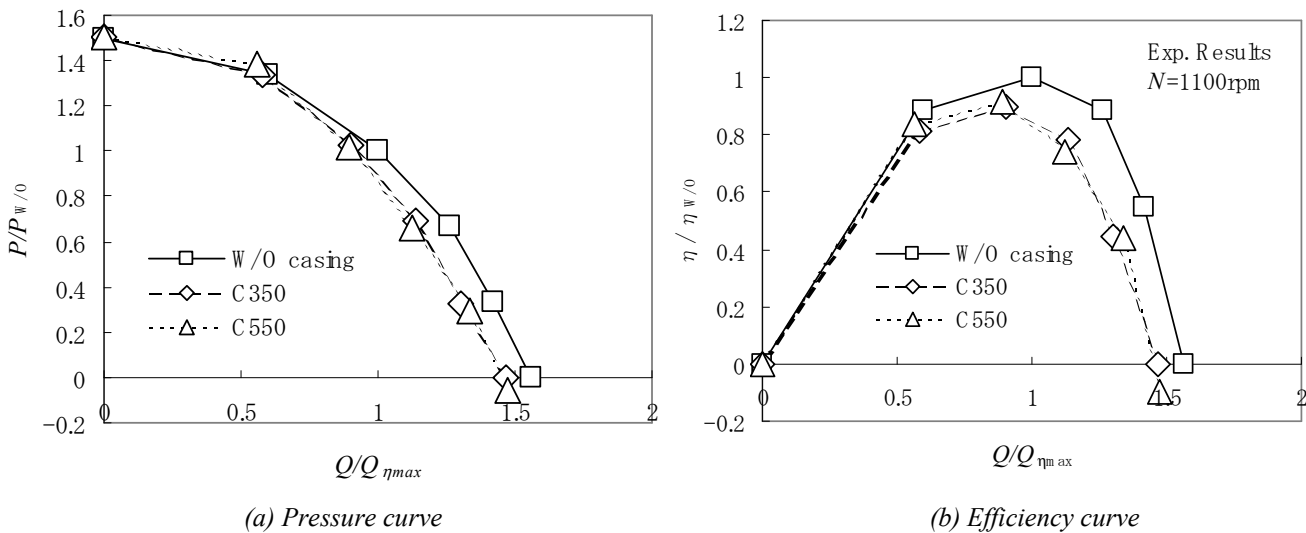

(a) Pressure curve   *(b) Efficiency curve*

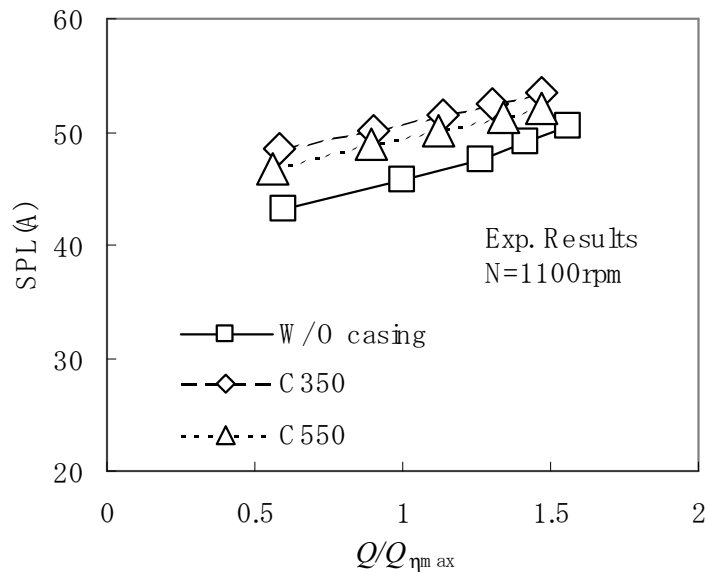*Figure 5: Performance curves (Experimental results)*

Figure 6: Noise performance curves (Experimental results)

Flow patterns of casing fan

Figure 7 shows the velocity vectors of C350 fan. The light colored vectors indicate the large velocities. The center figure is the section of mid-span. The flow out of the impeller is fairly distorted. The outflow from the impeller is very large between A and B, but is small between C and D. The flow at the inlet of the impeller that is observed near the center of the impeller is also distorted. The flow in the casing is almost rotating in clock-wise. It can be seen a little reverse flow at the back wall corners. The outflow from the casing is concentrated near the section A. The flow patterns at each section of A to D are shown. It is seen that the outflow from the impeller is large at the section A. The outflow from the impeller at section B is smaller than at section A.
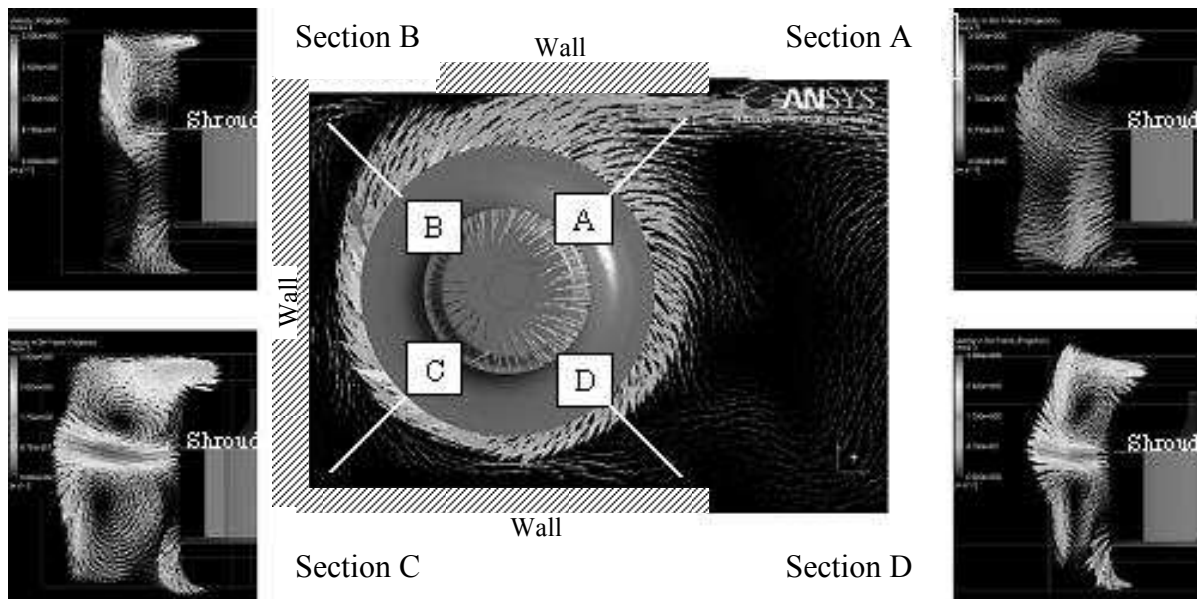

Figure 7: Velocity distributions in the fan(simulation results)

The flow out of the impeller is gathered near the upper and the lower shroud. The strong secondary circulating flow is generated near the shroud. At section C, the strong jet flow from the impeller is generated near the front shroud. Then it is generated the large and strong circulating flow near the upper shroud and the mid-span. The outflow from the impeller is small at the mid-span. At the section D, the flow out of the impeller is distorted toward to the upper shroud. The outflow from the impeller near the mid-span and hub is very small likely to the section C. There also exist the strong circulating flow at the upper shroud and the mid-span.

Figure 8 (a), (b) show the contour maps of the pressure and the velocity vectors in the impeller and the casing at mid-span for C350 fan. In figure (a), it can be seen the pressure drop near the leading edge of the impeller. This is corresponding to the large attack angle at the leading edge of the blade. As shown in figure 7, the flow into the impeller at the section IP2 to 4 is small. At the section of IP5 to 7 and 1, it is not emerged the large pressure drop at the leading edge of the blade. The pressure is varied very much in the casing. The pressure of the casing is large at the back wall compared to the outlet of the fan. The pressure near the corner at the back wall is large. The pressure rise in passage of the blade is large at these back locations, because the inflow to the blade is small as shown in figure7. The pressure becomes low at the outlet of the casing IP6. Figure (b) is the vector map of the velocities. In the impeller, the relative velocities are presented and the absolute velocities are presented in the casing. At the IP2 to 4, it is shown the large separated region near the trailing edge of the suction side. This is caused by the large pressure rise in the impeller. There exist the large velocity regions out of the impeller at IP5 and 6. The flow becomes large toward to the outlet of the fan. At the region, the pressure in the casing is low as shown in figure (a). At the other parts of the
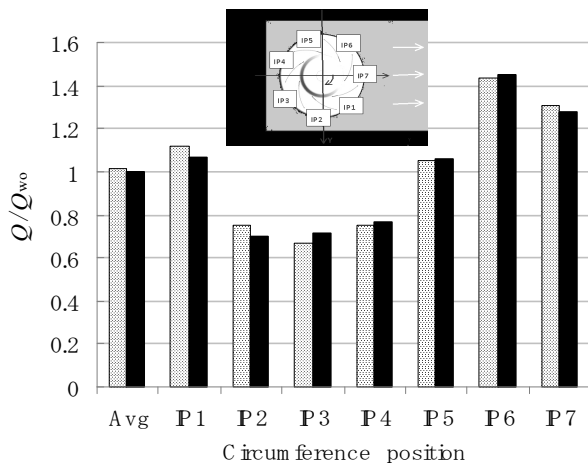
outlet of the fan, IP7 and IP1, the velocities are not so large. These distorted flow patterns are the typical feature of the square and rectangular casing. At IP1, the flow out of the impeller is divided toward to the fan exit and the back wall of the casing.
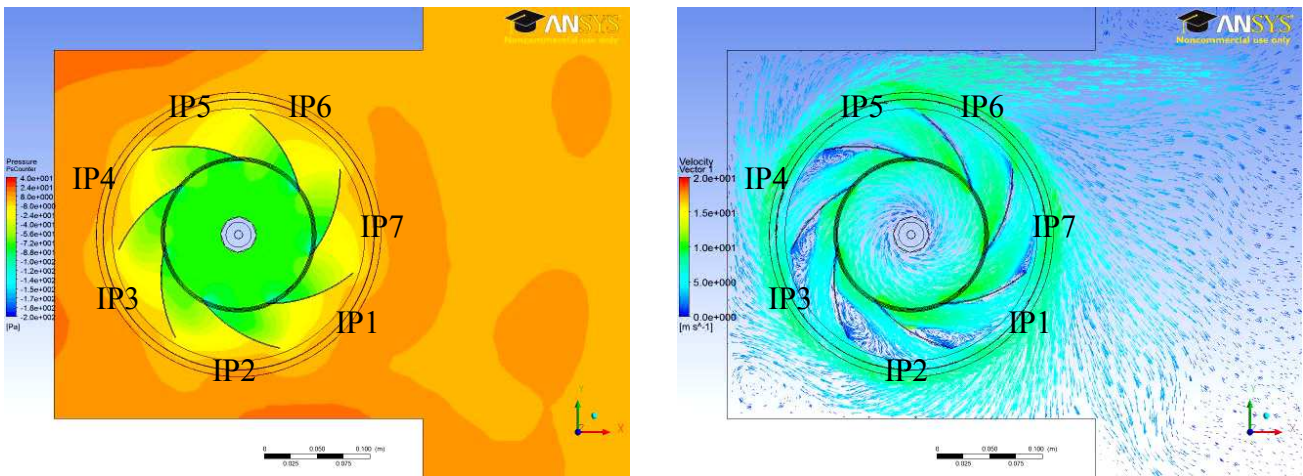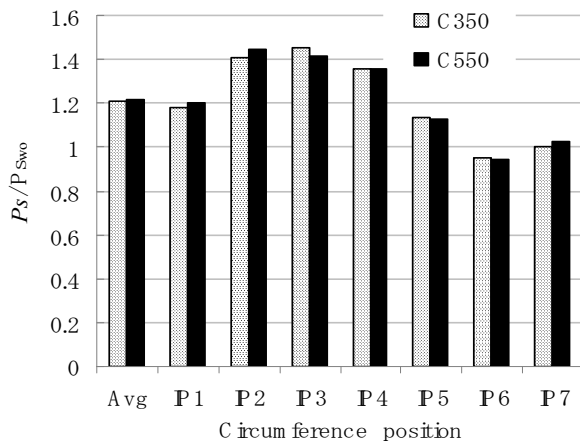

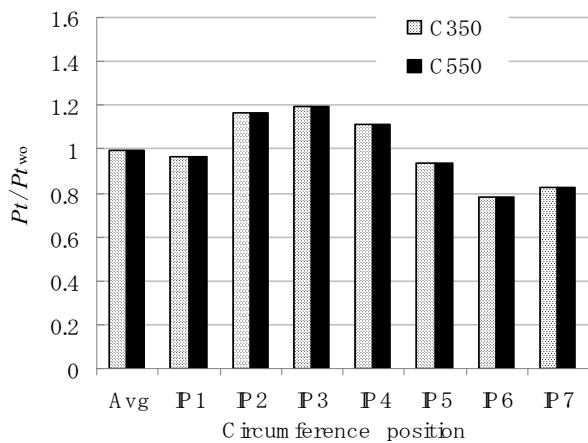*(a) Pressure distribution*   *(b) Velocity Vector*

Figure 8: Flow characteristics in C350 fan (Simulation results)
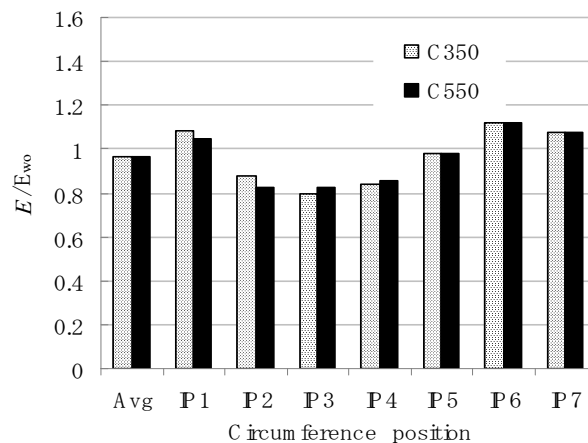

(*a*) *Flow rate*   *(b) Static pressure*

(c) Total pressure   *(d) Energy out of impeller*

Figure 9: Circumferential distributions of flow characteristics out of impeller (Simulation results)

Figure 9 shows the flow characteristics out of the impeller at each pitch locations. They are normalized by the value at maximum efficiency of the without casing fan. Figure (a) shows the flow rate out of the impeller. It is seen that the flow rate is small at the section IP2 to 4 and very large at IP 6 and 7. The value at IP6 is about twice at IP2 to 4. The distribution is corresponding to inflow distribution at the bell-mouth in figure 7. Figure (b) shows the pressure distribution. The static pressure is high at IP2 to 4 and low at IP6 and 7. This distribution is opposite to the flow rate distribution in figure (a). The averaged pressure is 20 percent higher than the without casing fan. The maximum pressure at IP2 and 3 is about 1.5 times higher than the minimum one at IP6. This is caused by the flow distribution shown in figure 8(a). As shown in figure 5(a), the pressure out of the impeller is increased with the flow rate decreasing. Then the small flow rate at IP2 to 4 makes the pressure out of the impeller large. Figure (c) shows the total pressure distribution. The total pressure becomes large at IP2 to 4. This distribution is similar to the static pressure. But the difference of maximum and minimum level is small compared with the static pressure distribution. The pitch-wise averaged value is almost same to the without casing fan. Figure (d) shows the energy from the impeller. The energy E is calculated by the multiple of the flow rate and the total pressure.

$$E = Q \times Pt \quad [\text{W}] \tag{1}$$

The distribution is similar to the flow rate of figure (a), because of the distortion of the flow rate being larger than the total pressure. The averaged energy is a little lower than the without casing fan.
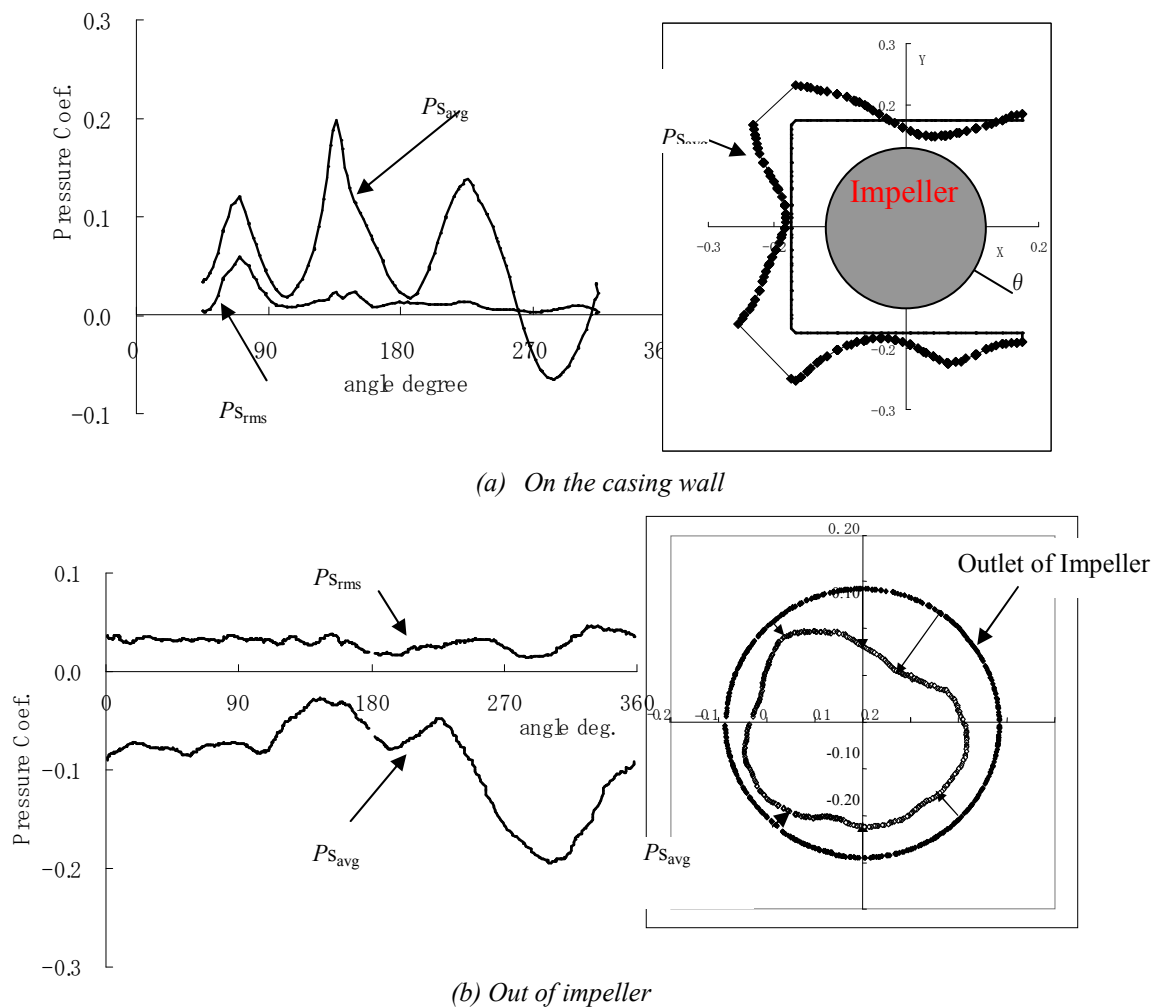

(a) On the casing wall

(b) Out of impeller

Figure10: Circumferential distributions of averaged and RMS pressure

(Simulation results)

Circumferential distribution of pressure and noise characteristics

Figure 10 shows the circumferential distribution of the time averaged and RMS pressures. Figure(a) is on the casing wall. The distribution of the averaged pressure has three peaks at 70, 135 and 225 degrees. The peak at 70 degree is corresponding to the interaction between the outflow from the impeller and the flow in casing. The locations of the peaks at 135 and 225 degrees are corresponding to the corner of the casing, shown in figure 8(b). The section areas of the casing are large at these locations and the flow in the casing decreases by the diffuser effect. The pressure fluctuation Ps_{rms} is large at 70 degree. The fluctuation is almost constant at the other angles. Figure(b) is the pressure at the outlet of the impeller. This distribution is different to the distribution at the casing wall. The pressure is almost constant during 0 to 225 degree and large up to the 225 degree. This distribution is similar not to the casing wall, but to the inflow distribution shown in figure 7. The pressure distribution out of the impeller is the single mode variation. It is remarkable that the circumferential pressure distribution out of the impeller is different to the casing wall.

Figure 11 shows the spectrum distribution of the sound pressure level of A-weighted. There exist the peaks at f=128, 256 and 384Hz. These peaks are corresponding to the interaction noise, nZ=1, and its harmonics, nZ=2, 3. The sound of nZ=1 is caused by the interaction between the inflow distortion and the blades. The peak level at 800Hz is the resonance in the casing and not relating to the flow in the fan, because the sound does not varied with the flow rate and other flow conditions.
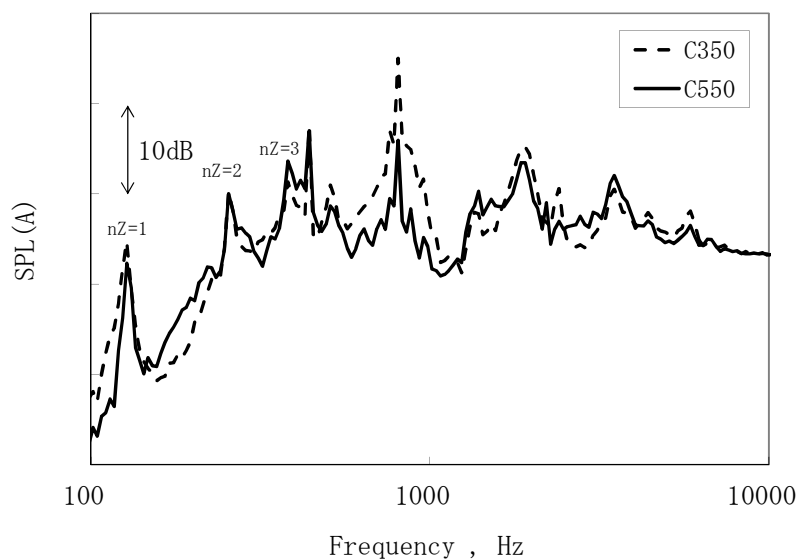

Figure11:Spectrum distribution of SPL , A-weight Characteristics
(Experimental results)

CONCLUSIONS

The flow characteristics were investigated for the backward curved centrifugal fan with experiments and simulations. The following results are obtained:

1. The decrement of the performance with rectangular casing fan becomes large at large flow rate. The noise level becomes large at all flow rates. But the casing length is little influenced to the fan performance.

2. The velocity and the pressure are varied very much in the casing wall. The pressure becomes high at the back of the casing and low at the outlet of the casing.

3. The pressure distribution on the casing wall has three peaks that correspond to the section of the casing. The flow rate out of the impeller has one peak distribution that corresponds to the inflow distribution.

4. The sound pressure level is strongly influenced to the distortion of the inflow, but the geometry of the casing.

BIBLIOGRAPHY

[1]   N. Takeuchi, T. Kobayashi, K. Matsuda, K. Shimizu, *Air-Flow Path Design in 3-Dimensional Air-Flow Analysis fro Recessed-Ceiling Type Packaged Air-Conditioning*, Mitsubishi Heavy Industry Technical Review, Vol. 37, No 2, pp 70-73, **2000**

[2]   T. Yamasaki, T. Ohnishi, T. Hirakawa, *Numerical and Experimental Analysis of Three-Dimensional Flow Structure in Centrifugal Fan without Scroll Casing*, Proceeding of Japan Society of Mechanical Engineering, N° 024-1, pp. 33-34, **2002**

[3]   A. komatu, T. Iwata, Z. Zheng, T.Ohnishi, *Effect of the leading edge of turbofan on the noise*, Proceeding of Japan Society of Mechanical Engineering, No 07-11, pp 91-92, **2007**

[4]   L. Chunxi, W. S. Ling, J. Yakui, *The performance of a centrifugal fan with enlarged impeller, Energy Conversion and Management*, Vol 52, pp 2902-2910, **2011**

[5]   A. Behzadmehr, J.B. Piaud, R. Oddo, Y. Mercadier, *Aero-Acoustical Effects of Some Parameters of a Backward-Curved Centri- fugal Fan Using DoE*, HVAC & Research, 12-2, pp 353-365, **2006**

[6]   Y. Yokoi, S. Inagaki, *Experimental Study of Flow Feature in a Spiral Casing of Turbo Fan*, Turbo-Machinery, Vol.33, No.4, pp 241-249, **2005**

[7]   S. Yamasaki, S. Komatsu, T. Obata, S. Yokoyama, *Investigation of Flow Pattern in a Backward-Curved Fan and Influence of Its Fan Shape on the Performance and Noise*, JSME B, Vol.65, No 636, pp 2770-2776, **1999**

[8]   K. Yamamoto, M. Kawahashi, *Simple 3D Numerical Analysis of Flow in a centrifugal Fan*, Trans. JSME B,   Vol.61, No. 584, pp 1418-1423, **1995**

[9]   D. Qi, Y. Zhang, S. Wen, Q. Liu, *Measurement and analysis of three- dimensional flow in a centrifugal fan volute with large volute width and rectangular cross-section*, ImechE 220A (J.Power & Energy), pp 133-153, **2006**